Environ Earth Sci (2016) 75:397
DOI 10.1007/s12665-016-5248-7

ORIGINAL ARTICLE

Changes in fluid flux and hydraulic head in a geothermal confined aquifer

Jingbo Zhao[1,2] · Xun Zhou[1,3] · Yuan Yu[1,4] · Chuanxia Ruan[1,5] · Xiaocui Wang[1] · Jingwei Li[1] · Qingxiao Zhang[1] · Xiaowei Shen[1]

Received: 6 December 2014 / Accepted: 4 November 2015 / Published online: 24 February 2016

Abstract Understanding the changes in fluid flux and hydraulic head in a confined aquifer where heat flow from below exists is important in the development of a geothermal field of basin-type. A 3D mathematical model describing thermal groundwater flow and heat transport is established. The partial differential governing equations are solved with the standard Galerkin finite element method and the streamline upwind Petrov–Galerkin method. Two cases of temperature differences between the bottom and upper boundaries are considered and one case of hydraulic gradient difference between the left and right boundaries are also examined. The numerical results show that when the temperature of the aquifer is under normal temperature and the temperatures of the top boundary are 45, 50 and 55 °C with the temperature of the bottom boundary of 60 °C, the values of fluid flux through the vertical flow section are 1000, 2134, 2214 and 2295 m^3/d in Case 2, which are mainly affected by the dynamic viscosity u. When the temperature difference between the top and bottom boundaries increases, the hydraulic gradient in x direction slightly increases with the increasing temperature difference. When the temperature differences are 15, 10, 5 and 0 °C, respectively, the hydraulic gradients are 0.01005, 0.01003, 0.01002 and 0.01 in Cases 1 and 2, and almost keep the same value of 0.01 under normal temperature. The hydraulic head in z direction obeys a nonlinear change and can be described with a 2nd order polynomial function.

Keywords Thermal groundwater · Temperature · Hydraulic head · Flow flux · Finite element method

Introduction

It is well known that in a horizontal, homogeneous and isotropic confined aquifer under normal temperature, fluid flux meets Darcy's law and hydraulic head linearly changes in the flow direction. In Fig. 1a if the confined aquifer has the width B and under normal temperature, the hydraulic head H will decrease linearly or the hydraulic gradient will keep constant in x direction, and the fluid flux Q_a through any vertical flow section under a steady-state condition can be calculated using $Q_a = KMB(H_1 - H_2)/L$ (Bear 1972, 1979). Nevertheless, when heat flow from below exists as shown in Fig. 1b, whether the flow flux Q_b and the hydraulic gradient keep the same as those in Fig. 1a and whether the hydraulic head H meets the linear variation in x direction are seldom examined. The focus of this work is on the effect of temperature on fluid flux and the hydraulic head variation in a geothermal confined aquifer system.

✉ Xun Zhou
zhouxun@cugb.edu.cn

1 School of Water Resources and Environment, China University of Geosciences (Beijing), Xueyuan Road 29, Beijing 100083, People's Republic of China

2 Beijing Research Institute of Uranium Geology (BRIUG), 10, Xiao-Guan-Dong-Li, P.O. Box 9818, Beijing 100029, People's Republic of China

3 Key Laboratory of Groundwater Circulation and Evolution, Ministry of Education, China University of Geosciences (Beijing), Xueyuan Road 29, Beijing 100083, People's Republic of China

4 Beijing Geology Prospecting and Developing Bureau, No.123 West 4th Ring North Road, Beijing 100195, People's Republic of China

5 Tianjin Geothermal Exploration and Development-Designing Institute, Weiguo Road 189, Tianjin 300250, People's Republic of China

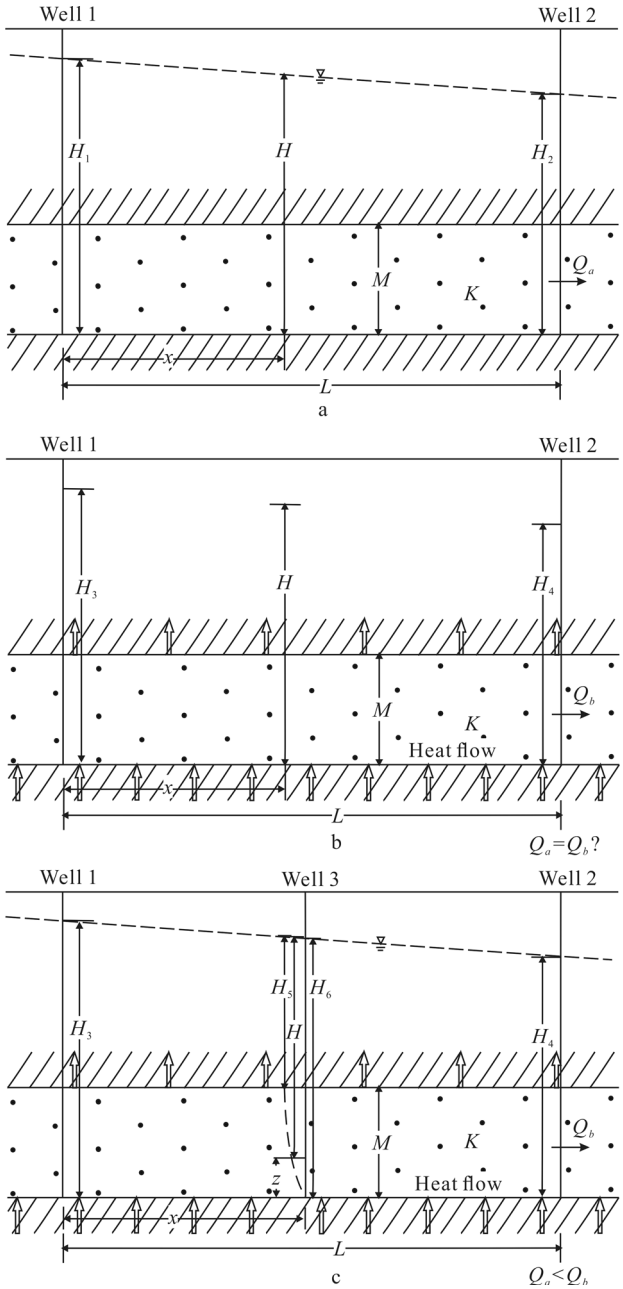

Fig. 1 Schematic profiles showing groundwater flow in x direction in a horizontal, homogeneous and isotropic confined aquifer with width B under a steady-state condition **a** under normal temperature, **b** when the heat flow from below is present and **c** the hydraulic head in x and z direction when the heat flow from below is present

Thermal groundwater in porous media is thought to be density-dependent flow, which has been studied extensively because of its important theoretical and practical applications. Fluid density gradients and dynamic viscosity resulting from variations in temperature play a significant role in flow and heat transport in groundwater systems (Simmons et al. 2001; Diersch and Kolditz 2002; Simmons et al. 2010; Ataie-Ashtiani et al. 2014). A large number of numerical studies have used the Elder problem (Elder 1967) as an example of density-dependent flow. It has been widely used as an unstable density-dependent flow benchmark problem (Voss and Souza 1987; Diersch and Kolditz 2002; Simpson and Clement 2003; Woods and Carey 2007; Ataie-Ashtiani et al. 2014). However, the case in Fig. 1b is seldom examined.

For a geothermal system, the density and dynamic viscosity of thermal groundwater are affected by temperature (Diersch 2005b). Therefore, the governing equation of thermal groundwater flow is different from that of constant-density flow under normal temperature. For thermal groundwater flow, there are two common forms of the governing equation. One is that the equivalent hydraulic head in the reference condition is defined to describing thermal groundwater, which can reflect the hydraulic changes affected by temperature (Diersch 2005b; Post et al. 2007). The other is that the pressure is adopted as the main variable (Kipp 1987; Pruess et al. 1999; COMSOL 2013). Both equations are deprived by the conservation law of continuum mass in porous media. For heat transport in a geothermal system, there are also two forms of the governing equation which are of the convective form and the divergence form (Kipp 1987; Pruess et al. 1999; Diersch 2002). The convective form is more common and is different from the divergence form when dealing with boundary conditions by using the finite element method (Diersch 2002). Considering the effect of the temperature on the density and dynamic viscosity, the appropriate analytical solution describing the thermal groundwater flow in Fig. 1b is hardly achieved (Wang 2011). Therefore, the numerical method is put forward and widely applied to describe the groundwater flow because of the great flexibility in handling complex problems. Many numerical codes have been developed, such as MODFLOW, TOUGH 2, FEFLOW (Voss 1984; Brebbia and Zamani 1989; Pruess et al. 1999; Harbaugh 2005; Diersch 2005b).

In this paper, the equivalent hydraulic head in the reference condition in the governing equation of thermal groundwater flow and the convective form of heat transportation are adopted. The system of governing equations and the Darcy's velocity are solved by means of the standard Galerkin finite element and streamline upwind Petrov–Galerkin method (SUPG). An emphasis is placed on the effect of the temperature on fluid flux through the vertical flow section and the equivalent hydraulic head variation in the x, y and z directions in different cases in a steady-state condition in the geothermal system shown in Fig. 1c. Knowledge of the flow flux and hydraulic head change in a geothermal confined aquifer is helpful in understanding the principle of groundwater movement in a groundwater system and is important in guiding the exploitation and utilization of thermal groundwater.

Mathematical models

For thermal groundwater, especially in deep-seated aquifers, the temperature is relatively high and changes greatly. The density and dynamic viscosity of thermal groundwater can be expressed as a function of temperature ignoring the effect of pressure and total dissolved solids on the thermal groundwater. Therefore, two factors should be considered in depriving the equations describing the thermal groundwater flow (Diersch 2005b). The general form of the Darcy's law describing the flow rate in a geothermal system is:

$$q = -\frac{k}{u}(\nabla p + \rho g \nabla z) \tag{1}$$

where q is the Darcy's velocity whose components along x, y and z directions are q_x, q_y and q_z (L T^{-1}), k is components of the permeability tensor (L^2), u is the dynamic viscosity, p is the fluid pressure (M L^{-2} T^{-2}), ρ is the fluid density (M L^{-3}), g is the gravitational acceleration (LT^{-2}), z is the elevation above the datum (L).

In a geothermal system the equivalent hydraulic head under the reference condition can be defined as (Lusczynski 1961; Post et al. 2007):

$$H = \frac{p}{\rho_0 g} + z \tag{2}$$

where ρ_0 is the density under the reference condition defined for a fixed temperature (M L^{-3}).

The reference hydraulic conductivity K [L T^{-1}] and the dynamic viscosity difference ratio u_r are introduced:

$$K = \frac{\rho_0 g k}{u_0} \tag{3}$$

$$u_r = \frac{u}{u_0} \tag{4}$$

where u_0 is the dynamic viscosity under the reference condition.

By substituting Eqs. (2), (3), and (4) into Eq. (1), we obtain the Darcy's velocity in the geothermal system as follows:

$$q = -\frac{K}{u_\mathrm{r}}(\nabla H + \rho_\mathrm{r} \nabla z) \tag{5}$$

where $\rho_r = (\rho - \rho_0)/\rho_0$ is the density difference ratio. This equation represents two driving forces that cause thermal groundwater flow, the equivalent hydraulic head differences that originate from the topographic relief on the water table, and a buoyancy force caused by density differences of the fluid. Furthermore, the dynamic viscosity difference ratio u_r play an important role in thermal groundwater, which is usually neglected for solute transport equations (Ophori 1998).

According to Eq. (5), the fluid flux Q (L^3 T^{-1}) through the flow section in a geothermal system can be expressed as:

$$Q = n \cdot q \cdot S \tag{6}$$

where n is the directed positive outward on S, S is the area of the flow section (L^2).

According to the universal principle of conservation, the mass conservation equation for thermal groundwater flow neglecting the source/sink can be written as (Bear 1972):

$$\frac{\partial}{\partial t}(\rho\phi) + \nabla \cdot (\rho q) = 0 \tag{7}$$

where ϕ is the porosity [−].

Introduce the reference specific storage coefficient, S_0 (L^{-1}):

$$S_0 = \rho_0 g[(1-\phi)\alpha + \beta\phi] \tag{8}$$

Substituting Eqs. (2), (3), (5) and (8) into Eq. (7), the governing equation for thermal groundwater flow can be deprived:

$$S_0(1+\rho_r)\frac{\partial H}{\partial t} + \frac{\phi}{\rho_0}\frac{\partial \rho}{\partial T}\frac{\partial T}{\partial t} - \nabla \cdot \left[\frac{K(1+\rho_r)}{u_r}(\nabla H + \rho_r \nabla z)\right] = 0 \tag{9}$$

According to the energy conservation of a geothermal system, the transport equation for the heat in which the sink/source is neglected can be expressed as (Bear 1972; Diersch 2005b):

$$[\phi\rho C_\mathrm{f} + (1-\phi)\rho_\mathrm{s} C_\mathrm{s}]\frac{\partial T}{\partial t} + \rho C_\mathrm{f} q \nabla T - \nabla \cdot (\lambda \cdot \nabla T) = 0 \tag{10}$$

where ρ_s is the density of solid particles [ML^{-3}], T is the temperature [Θ], C_f is the specific heat capacity of water (J M^{-1} Θ^{-1}), C_s is the specific heat capacity of solid particles (J M^{-1} Θ^{-1}). λ is the tensor of the hydrodynamic-thermo-dispersion (J L^{-1} T^{-1} Θ^{-1}).

Several relations are reported in the literature describing the dependence of fluid viscosity and density on temperature (Smith and Chapman 1983; Heggen 1983; Diersch 2005b). We have chosen to use two of the more simple models, given as:

$$\rho = \rho_0[1 - \overline{\beta}(T)(T - T_0)] \tag{11}$$

$$u_\mathrm{r} = \frac{1 + 0.7063\xi_{(T=T_0)} - 0.04832\xi^3_{(T=T_0)}}{1 + 0.7063\xi - 0.04832\xi^3} \tag{12}$$

with $\xi = (T - 150)/100$ at T (°C), where $\overline{\beta}(T)$ is the fluid expansion coefficient and T_0 indicates the reference values of temperature.

To close the set of the governing equations the tensor of the hydrodynamic–thermo-dispersion λ is given by (Diersch 2005b):

$$\lambda = \lambda^{\text{cond}} + \lambda^{\text{disp}},\ \lambda^{\text{cond}} = [\phi\lambda^{\text{f}} + (1-\phi)\lambda^{\text{s}}]\delta_{ij},$$
$$\lambda^{\text{disp}} = \rho C_{\text{f}}[\alpha_T|q|\delta_{ij} + (\alpha_L - \alpha_T)\frac{q_i q_j}{|q|}] \quad (13)$$

where $\lambda^{\text{f}}, \lambda^{\text{s}}$ are the thermal conductivity of the water and solid phase, respectively, and α_L, α_T are the longitudinal and transverse thermodispersivity $|q|$ is the absolute specific Darcy's fluid flux, δ_{ij} (Kronecker's delta) is equal to 1 if $i = j$, otherwise it is equal to zero.

Finite element formulation

Equations (5) and (10) are approximated using the Galerkin finite element technique. The procedure of the Galerkin formulation is now standard and can be found in many references (Huyakorn et al. 1987; Diersch 2005a; Wang 2008). Thus, the final systems of differential equations that need to be solved are given below. The system of equations for fluid flow takes the following form:

$$O_{IJ}(dH_J/dt) + P_{IJ}(dT_J/dt) + S_{IJ}H_J - F_I = 0 \quad (14)$$

$$A_{IJ}q_J = B_I \quad (15)$$

where the subscripts $I, J = 1, \ldots, M$, denoting nodal indices; H_J are nodal equivalent hydraulic head values; T_J are nodal temperature values; q_J are nodal velocity values; M is the number of nodes in the finite element network, and O_{IJ}, S_{IJ}, F_I, P_{IJ}, A_{IJ} and $\boldsymbol{B_I}$ are matrices given by $O_{IJ} = \sum_e \int_{\Omega^e} S_0(1+\rho_{\text{r}})N_I N_J$, $\boldsymbol{S_{IJ}} = \sum_e \int_{\Omega^e} \frac{K_{ij}(1+\rho_r)}{u_r}\frac{\partial N_I}{\partial x_i}\frac{\partial N_J}{\partial x_j}$, $F_I = \sum_e \int_{\Gamma^e} N_I n \cdot q - \sum_e \int_{\Omega^e} \frac{K_{ij}\rho_{\text{r}}(1+\rho_{\text{r}})}{u_{\text{r}}}\frac{\partial N_I}{\partial x_i}\frac{\partial y}{\partial x_j}$, $P_{IJ} = \sum_e \int_{\Omega^e} \frac{\phi}{\rho_0}\frac{\partial \rho}{\partial T}N_I N_J$, $A_{IJ} = \sum_e \int_{\Omega^e} N_I N_J$, $B_I = -\sum_e \int_{\Omega^e} \frac{K_{ij}}{u_{\text{r}}}\frac{\partial N_J}{\partial x_j}H_J N_I - \sum_e \int_{\Gamma^e} \frac{K_{ij}\rho_{\text{r}}}{u_{\text{r}}}\frac{\partial y}{\partial x_j}N_I$

where Ω^e is the spatial domain of the element, Γ^e is the boundary of Ω^e, N_I, N_J are basis functions and n is the directed positive outward on Γ^e; $i, j = x, y, z$ are spatial indices of the Cartesian coordinates.

For the conduction–convection heat transfer Eq. (10), the numerical oscillation and inaccuracies may occur solved by the standard Galerkin method solution. Thus, another method is provided to handle this case which is the streamline upwind Petrov–Galerkin method (SUPG) (Brooks and Hughes 1982; Zienkiewicz and Wu 1992; Nadukandi et al. 2010). The matrix system of Eq. (10) for heat transportation can be expressed as

$$E_{IJ}(dT_J/dt) + U_{IJ}T_J - Q_{IJ} = 0 \quad (16)$$

with its components written in indicial notations:

$$E_{IJ} = \sum_e \int_{\Omega^e} [\phi\rho C_{\text{f}} + (1-\phi)\rho_{\text{s}}C_{\text{s}}]w_I N_J, U_{IJ} = \sum_e \int_{\Omega^e} \rho C_{\text{f}} q_i \frac{\partial N_J}{\partial x_i} w_I + \sum_e \int_{\Omega^e} \lambda_{ij}\frac{\partial w_I}{\partial x_i}\frac{\partial N_J}{\partial x_j}, Q_{IJ} = \sum_e \int_{\Gamma^e} w_I n \cdot (\lambda \cdot \nabla T)$$

It is found that the test function w_I of the form given below is optimal:

$$w_I = N_I + \frac{\alpha h}{2}\frac{u_x(\partial N_I/\partial x) + u_y(\partial N_I/\partial y) + u_z(\partial N_I/\partial z)}{|u|} \quad (17)$$

$$\begin{cases} u_x = \rho C_f q_x \\ u_y = \rho C_f q_y \\ u_z = \rho C_f q_z \end{cases} \quad (18)$$

$$|u| = \sqrt{u_x^2 + u_y^2 + u_z^2} \quad (19)$$

$$\alpha = \alpha_{opt} = \coth\frac{Pe}{2} - \frac{2}{Pe} \quad (20)$$

$$Pe = \frac{|u|h}{\lambda} \quad (21)$$

where h is the element size and here Pe is the element Peclet number.

For linear equations, quite a few methods have been developed, such as the Gauss–Seidel iteration method, the Gauss elimination method, the successive over relaxation method and so on (Li et al. 2005; Xue and Xie 2007). For nonlinear equations, the Picard iteration method is relatively common (Putti and Paniconi 1995; Huang et al. 1996). In this work, Eqs. (14) and (15) are solved by using the successive over relaxation method and Eq. (16) is nonlinear equation which is solved with the Picard iteration method. The numerical results have been verified with the software FEFLOW.

The geothermal confined aquifer

The horizontal, homogeneous and isotropic confined aquifer exists in China when the heat flow from below exists, as shown in Fig. 1b. The aquifers of this type are widely distributed in North China in confined aquifers of great depths in sedimentary basins and are of low-to-moderate temperature (Wang et al. 1993; Chen et al. 1994). For example, thermal groundwater with temperature ranging from 45 to 60 °C is found in the Tertiary sandstone aquifer system beneath the cities of Tianjin and Beijing (Zhou et al. 2001a, b). The aquifers of this type in China, which are composed mainly of sandstone and limestone, are of large range and thickness and can be considered to be infinite (Chen et al. 1994; Lin et al. 2013). Fluid flux and the equivalent hydraulic head of the middle part in these aquifers can be considered to be hardly affected by the boundary conditions if sources do not exist. In this paper, we place an emphasis on the features of fluid flux and the equivalent hydraulic head of the middle part in these

aquifers. Therefore, a 3D steady-state mathematical model can be established. The aquifer is assumed to be a horizontal, homogeneous and isotropic confined one consisting of sandstone which is schematically shown in Fig. 1. The modeled domain is assumed a rectangular of 10,000 × 1000 m and the thickness of the aquifer is 100 m. We focus on the middle part of the model, which ranges in the x axis from 4500 m to 5500 m.

The model domain is discretized by using 100 × 100 × 10 m cube in x, y and z directions with 10,000 elements. For heat flow, the top and bottom boundaries are boundary conditions of the first type, the values of which are T_1 and T_2. The other boundary conditions are assigned no-heat flow, which can be expressed as $n \cdot (\lambda \cdot \nabla T) = 0$. For water flow, the left and right boundary conditions are the first type, of which the values are H_1 and H_2 and zero flux boundary conditions are adopted for the other sides.

Considering the occurrence of thermal groundwater of low-to-moderate temperature in China, the following three cases are illustrated. In these cases, the effect of the temperature on fluid flux and the equivalent hydraulic head of thermal groundwater are examined. The reference temperature is equal to the normal temperature, which is given as 15 °C. The value of the reference hydraulic conductivity is 1.15741×10^{-5} m/s (1 m/d).

Case 1

In Case 1, an emphasis is placed on the effect of temperature on fluid flux and the equivalent hydraulic head. It is assumed that the temperature of the entire model is constant, which values are 40, 50 and 60 °C. The equivalent hydraulic heads of the left and right boundaries under the reference temperature are 1100 and 1000 m, respectively.

Case 2

Case 2 focuses on the effect of the temperature difference of the model on fluid flux and the equivalent hydraulic head. The equivalent hydraulic heads of the left and right boundaries under the reference temperature are 1100 m and 1000 m, respectively. The temperature of the bottom boundary is 60 °C. The temperature of the top boundary is changed, which values are in 45, 50 and 55 °C.

Case 3

Case 3 centers on the effect of the equivalent hydraulic head difference on fluid flux and the equivalent hydraulic head. The equivalent hydraulic heads of the left boundary are 1100, 1300 and 1500 m, respectively. The equivalent hydraulic heads of the right boundary remain unchanged, which value is 1000 m and the temperature of the top and bottom boundary are 45 and 60 °C. Except the values of parameters and boundary conditions mentioned above, the values of other parameters and boundary conditions which are kept unchanged in the simulation are listed in Table 1.

In the above cases, the profile in which y is equal to 500 m is chosen to examine the equivalent hydraulic head variation in x and z directions. For the equivalent hydraulic head in x direction, three lines in which z is equal to 100, 50 and 0 m are chosen in the profile. For the equivalent hydraulic head in z direction, three lines in which x is 4500, 5000 and 5500 m are chosen in the profile. The profile in which x is equal to 5500 m is chosen as the vertical flow section.

Results and discussions

In the paper the hydraulic head, the temperature and the Darcy velocities in x, y and z directions are obtained by using the finite element method. And the equation groups of the hydraulic head, the temperature and the Darcy velocities in x, y and z directions are solved by using the iteration methods. Therefore, the maximum tolerances of the iteration methods are needed. For the hydraulic head, the relative maximum tolerances are up to the magnitude order of 10^{-11}. For the temperature the relative maximum tolerances are up to the magnitude order of 10^{-9}, and for the Darcy velocities the relative maximum tolerance is up to the magnitude order of 10^{-13}. In fact for the hydraulic head and temperature, the five digits after decimal point of the numerical results are kept for figures and compared with the values of the hydraulic head and the temperature, the other digits after decimal point can be neglected.

Table 1 Basic parameters for the numerical simulations

Quantity	Value
Length of the modeled domain (L)	10,000 m
Thickness of the modeled domain (M)	100 m
Width of the modeled domain (B)	1000 m
Porosity (ϕ)	0.03
Gravitational acceleration (g)	9.81 ms^{-2}
Thermal conductivity of the water (λ^f)	0.65 Jm^{-1} s^{-1} K^{-1}
Thermal conductivity of the solid phase (λ^s)	2.6 Jm^{-1} s^{-1} K^{-1}
Longitudinal thermodispersivity (α_L)	0 m
Transverse thermodispersivity (α_T)	0 m
Density of solid particles (ρ_s)	2600 kg m^{-3}
Specific heat capacity of solid particles (C_s)	878 J kg^{-1} K^{-1}
Specific heat capacity of water (C_f)	4200 J kg^{-1} K^{-1}

For the equivalent hydraulic head in x direction, Figs. 2, 3, 4 show that the equivalent hydraulic head has a linear decrease with the increasing x in Case 1. When the temperature of the whole aquifer is 40, 50 and 60 °C, respectively, the slopes of the three lines in x direction are 0.01, which is just equal to the hydraulic gradient in the aquifer under normal temperature. The result indicates that when the left and right boundary conditions of the aquifer are determined, the temperature of the aquifer has no influence on the hydraulic gradient in Case 1. This phenomenon keeps consistent with the aquifer under normal temperature.

For the equivalent hydraulic head in z direction, Figs. 2, 3, 4 indicate that when the elevation z decreases, the equivalent hydraulic head decreases linearly in Case 1. When the temperature of the whole aquifer increases, the slopes of the three lines in z direction also increase. For example, when the temperature is 40, 50 and 60 °C, the values of the slopes are 0.0069, 0.0111 and 0.0159. This phenomenon is different from the aquifer under normal temperature.

For the aquifer under normal temperature given as 15 °C, fluid flux through the flow section can be easily calculated by using Eq. (6), and the value is 1000 m^3/d. However, Fig. 5 shows that when the temperature of the whole aquifer increases, fluid flux through the vertical flow section also increases in Case 1. For example, when the temperature is 15, 40, 50 and 60 °C, the values of fluid flux are 1000, 1717, 2039 and 2378 m^3/d. This can be explained by using Eqs. (5) and (6). Firstly, Figs. 2, 3, 4 indicate that the hydraulic gradient in x direction remains unchanged when the temperature of the aquifer increases in Case 1. Secondly, the aquifer is assumed to be a homogeneous and isotropic confined aquifer. The reference hydraulic conductivity K and the area of the vertical flow section S are determined and the value of ∇z in x direction is equal to 0. Therefore, the last term u_r, which is affected by the temperature, is the unique factor to have direct influence on the fluid flux in Case 1. According to Eq. (4), it is found that the dynamic viscosity u is the unique factor to lead to the increase of the fluid flux. For example, when the temperature is 40 °C, the value of u_r is 0.5821 and the Darcy's velocity of each node in x direction is 0.01718 m/d, which can be solved by Eq. (5). The value of fluid flux through the vertical flow section is 1718 m^3/d, which is just equal to the value solved by Eq. (15). When the temperature is 50 and 60 °C, the same conclusions can be drawn that the dynamic viscosity u directly affected the fluid flux and the Darcy's velocity can also directly be solved by using Eq. (5). Therefore, in Case 1 when the temperature increases, the dynamic viscosity u decreases, which directly lead to the increase of Darcy's velocity and fluid flux.

Figures 6, 7, 8 show that the equivalent hydraulic head also varies linearly in x direction in Case 2. However, the slopes of the fitted lines are slightly different from that in Case 1. In Case 2, the slopes slightly increase with the temperature difference between the top boundary and the bottom boundary. For example, when the temperature

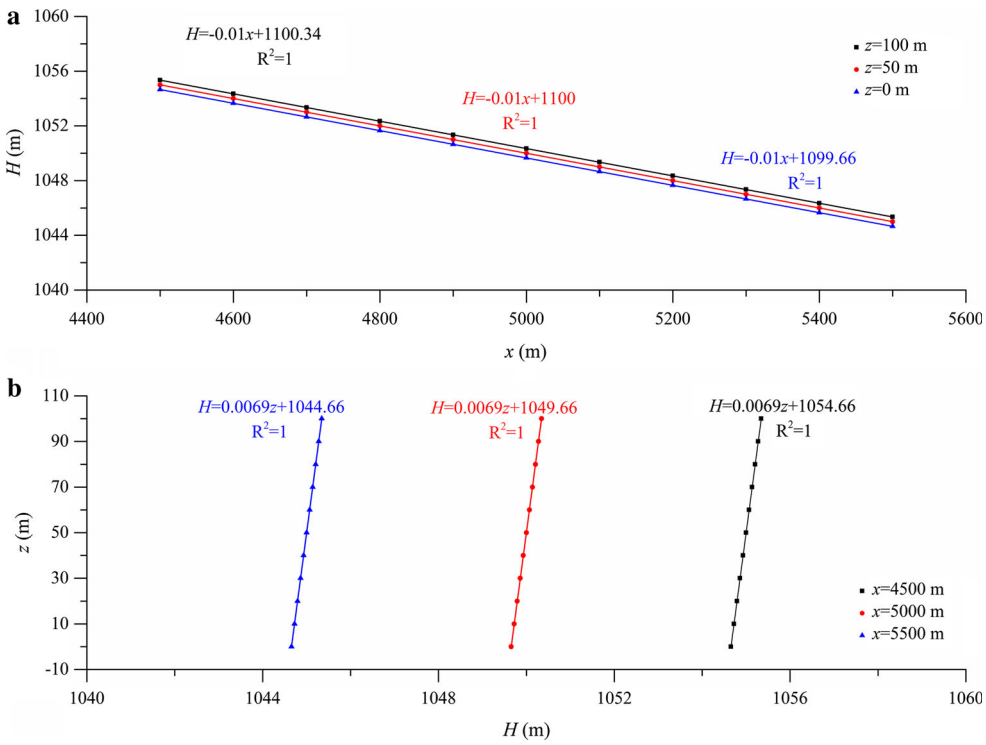

Fig. 2 Equivalent hydraulic head and fitted curves in Case 1 in which the temperature is 40 °C **a** in x direction and **b** in z direction

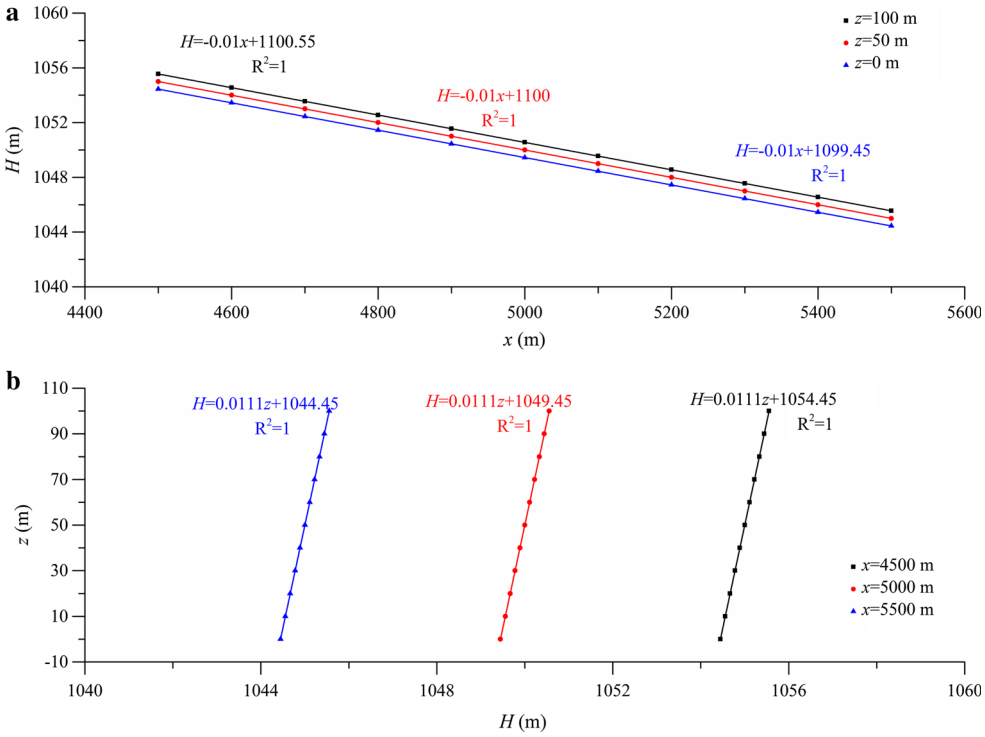

Fig. 3 Equivalent hydraulic head and fitted curves in Case 1 in which the temperature is 50 °C **a** in x direction and **b** in z direction

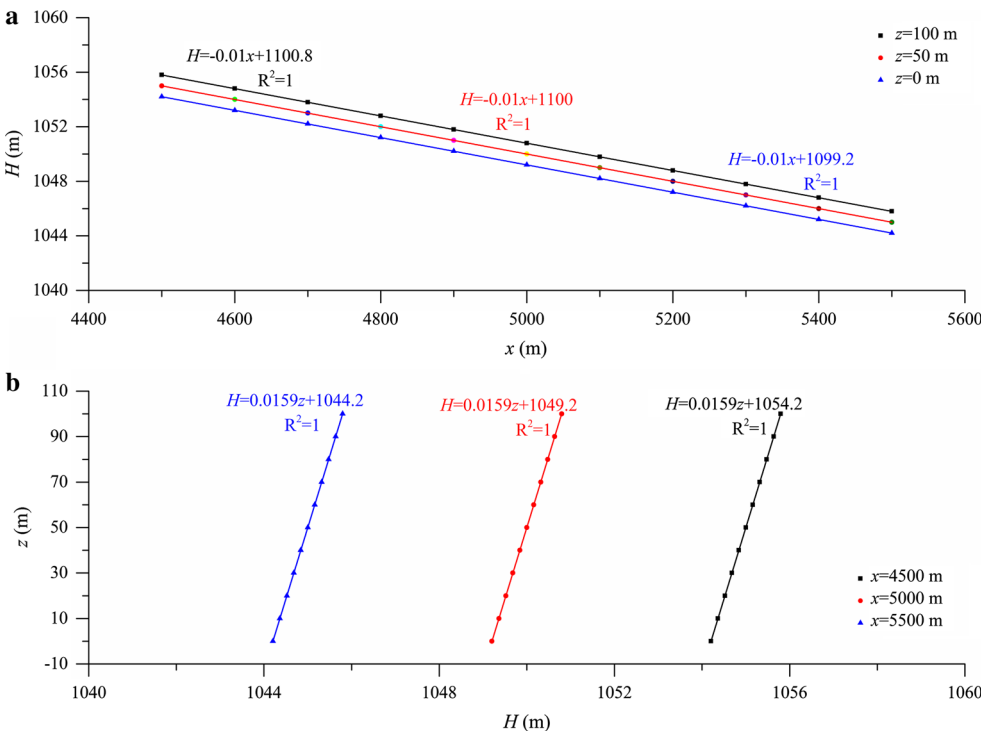

Fig. 4 Equivalent hydraulic head and fitted curves in Case 1 in which the temperature is 60 °C **a** in x direction and **b** in z direction

difference is 15, 10 and 5 °C, the slopes are 0.01005, 0.01003 and 0.01002. In contrast with the values of the equivalent hydraulic head in the mathematical model, the errors caused by the slopes can be neglected. It is also found that the slopes in x direction remain unchanged in different temperature of the top boundary in Case 2, which value is 0.01. Besides, the slopes of the three lines on which z is equal to 100, 50 and 0 m keep the same in z direction. This phenomenon shows that the slopes have no relationship with the elevation.

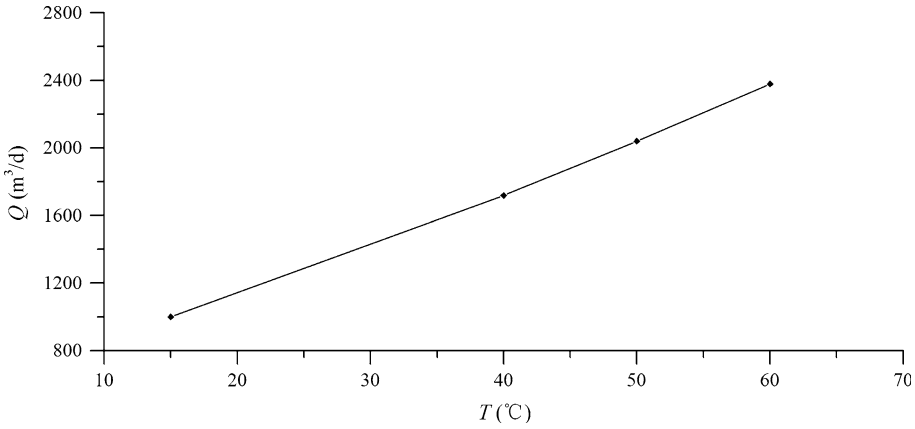

Fig. 5 The trend of fluid flux variation with the temperature in Case 1

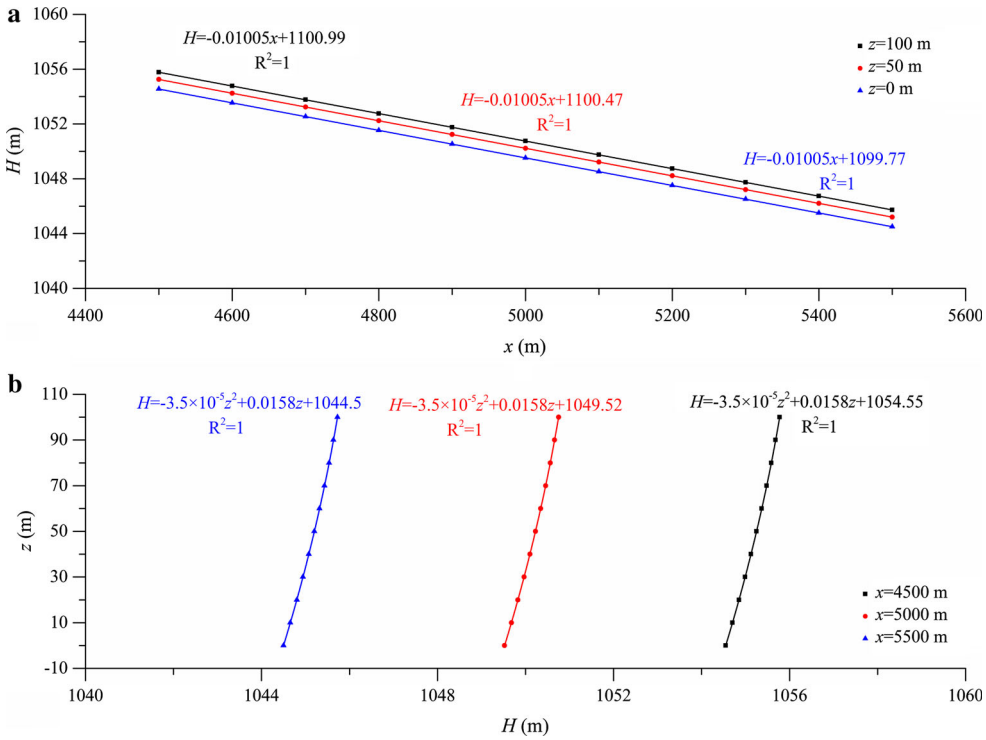

Fig. 6 Equivalent hydraulic head and fitted curves in Case 2 in which the temperature of the top boundary is 45 °C **a** in x direction and **b** in z direction

Figures 6, 7, 8 also indicate that in z direction the equivalent hydraulic head obeys nonlinear changes and increases with the elevation, which is different from that in Case 1 and that in the aquifer under normal temperature. This phenomenon can be described by using a 2nd order polynomial function. The fitted functions show that when the temperature difference between the top boundary and the bottom boundary is higher, this phenomenon is more obvious in Figs. 6, 7, 8. When the temperature difference decreases, the equivalent hydraulic head is close to the linear changes.

Figure 9 indicates that fluid flux through the vertical flow section increases with the temperature of the top boundary. The temperature difference between the top boundary and the bottom boundary in Case 2 is higher, the values of fluid flux is also higher. For example, when the temperature differences are 15, 10, 5 and 0 °C, the values of fluid flux are 2134, 2214, 2295 and 2378 m^3/d. The slopes in x direction are thought to remain unchanged when the temperature difference increases in Figs. 6, 7, 8. Therefore, the same conclusion can be drawn that Darcy's velocity and fluid flux are directly determined by the dynamic viscosity u, which is affected by temperature. The temperature decreases with the elevation in Case 2. Therefore, the Darcy's velocity of each node in x direction increases when the elevation decreases. For example, when the temperature of the top boundary is 45 °C, for the nodes of coordinates of (4500,500,100), (4500,500,50) and

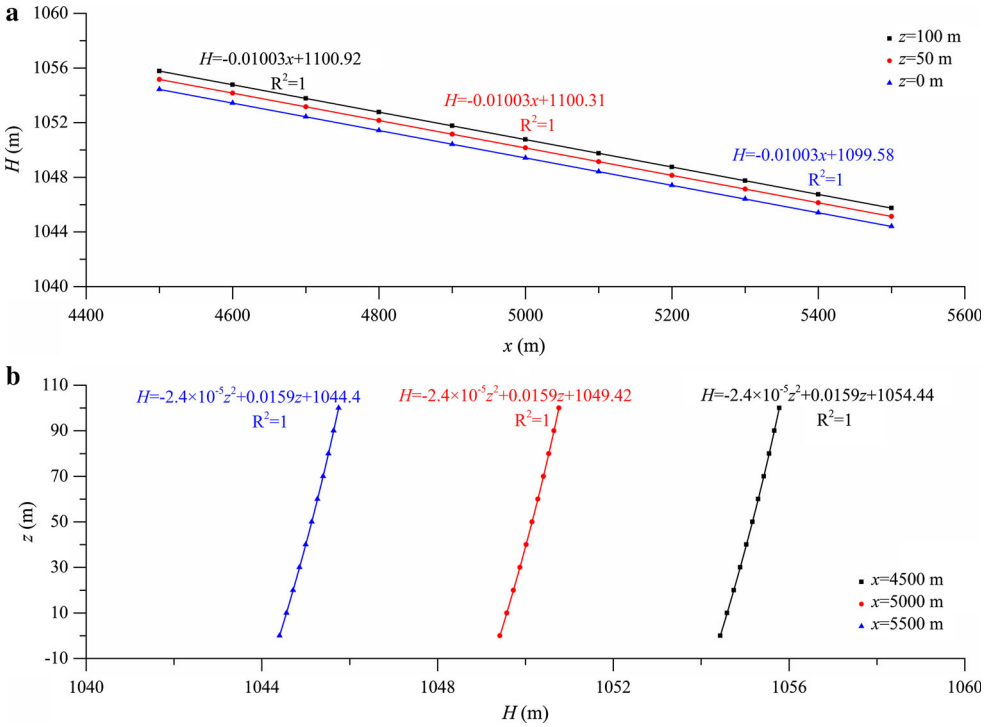

Fig. 7 Equivalent hydraulic head and fitted curves in Case 2 in which the temperature of the top boundary is 50 °C **a** in x direction and **b** in z direction

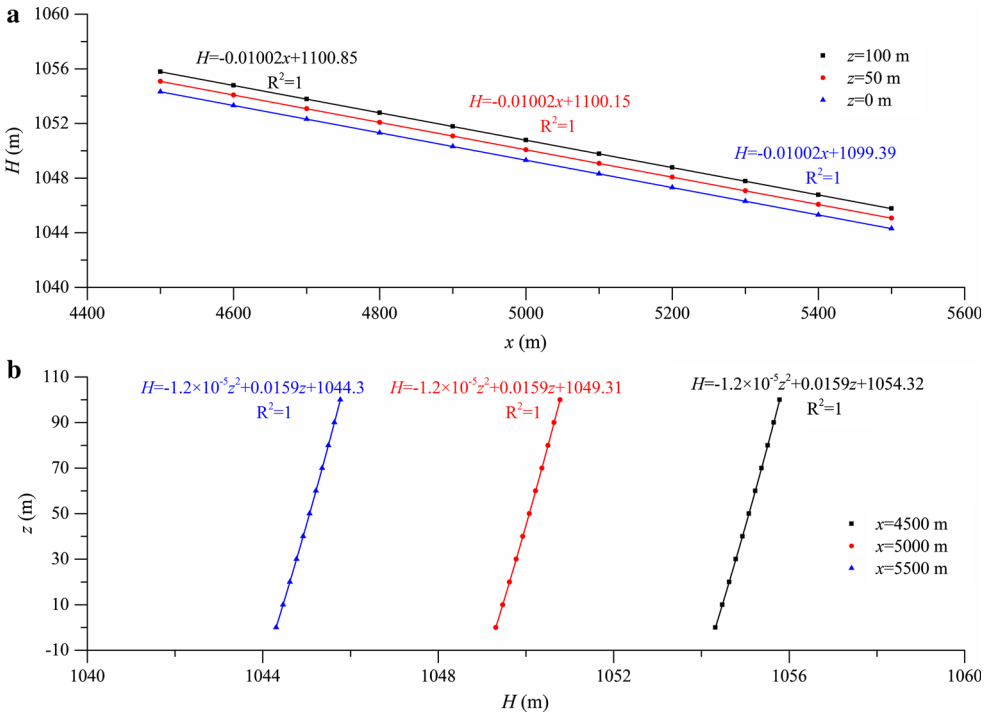

Fig. 8 Equivalent hydraulic head and fitted curves in Case 2 in which the temperature of the top boundary is 55 °C **a** in x direction and **b** in z direction

(4500,500,0), the Darcy's velocities are 0.019, 0.021 and 0.024 m/d.

Figures 6, 10, 11 indicate that when the equivalent hydraulic head difference between the left boundary and the right boundary enlarges 3 and 5 times, the equivalent hydraulic head also varies linearly in x direction and the hydraulic gradient also enlarge 3 and 5 times. For example, when the equivalent hydraulic head differences are 100, 300 and 500 m, respectively, the values of the hydraulic gradient are 0.01005, 0.03026 and 0.05044, which keep consistent with the aquifer under normal temperature. The equivalent hydraulic head in z direction also meets

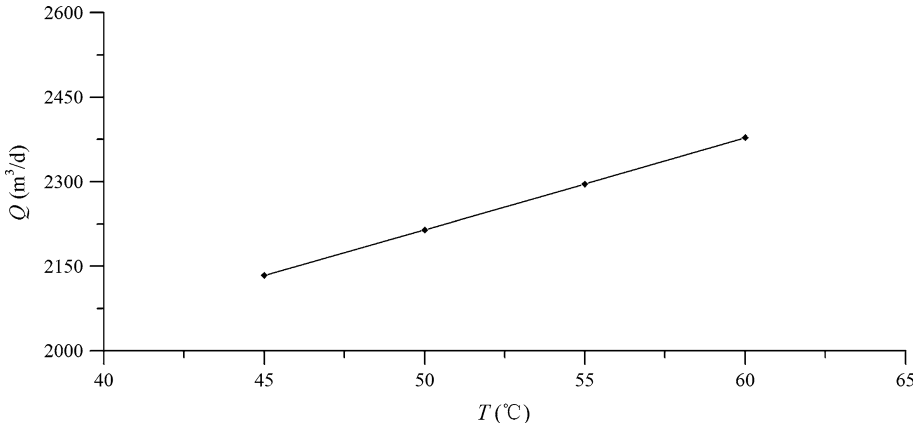

Fig. 9 The trend of fluid flux variation with the temperature of the top boundary in Case 2

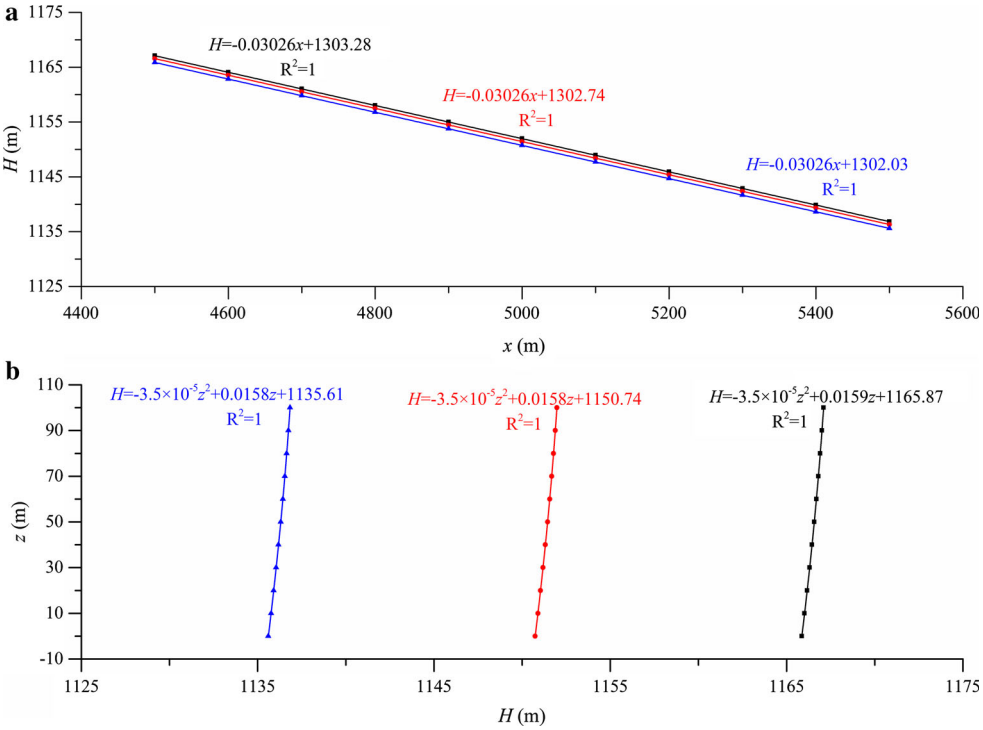

Fig. 10 Equivalent hydraulic head and fitted curves in Case 3 in which the equivalent hydraulic head of the left boundary is 1300 m **a** in x direction and **b** in z direction

nonlinear variation and increases with the elevation, which can be describes by a 2th order polynomial function as shown in Figs. 6, 10 and 11. When the values of the equivalent hydraulic head difference are 100, 300 and 500 m, the fitted functions do not remain unchanged, which are affected by the hydraulic gradient. Figure 12 shows that when the values of the equivalent hydraulic head are 1100, 1300 and 1500 m, the fluid flux through the vertical flow section linearly increases, which keep consistent with the aquifer under normal temperature. Therefore, fluid flux through the vertical flow section increases linearly with the hydraulic gradient in the geothermal confined aquifer system.

Thus, for a horizontal, homogeneous and isotropic confined aquifer, the flow flux Q_b is greater than Q_a in the aquifer under normal temperature, the equivalent hydraulic head H meets a linear variation in x direction and a non-linear variation in z direction, and the hydraulic gradient almost remains unchanged when the heat flow from below is present in a steady-state condition shown in Fig. 1c.

Conclusions

The numerical results of a 3D steady-state mathematical model show that the fluid flux through the flow section increases with the temperature and is larger than that in the confined aquifer under normal temperature. The equivalent hydraulic head decreases linearly with the increase of x in x direction and the equivalent hydraulic head obeys

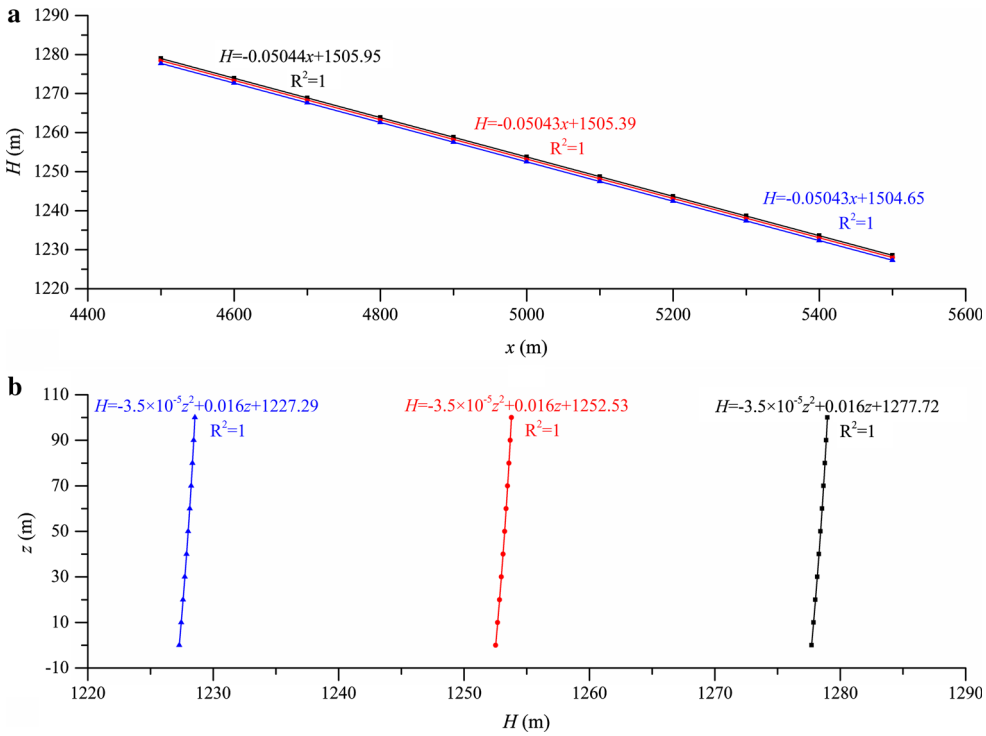

Fig. 11 Equivalent hydraulic head and fitted curves in Case 3 in which the equivalent hydraulic head of the left boundary is 1500 m **a** in x direction and **b** in z direction

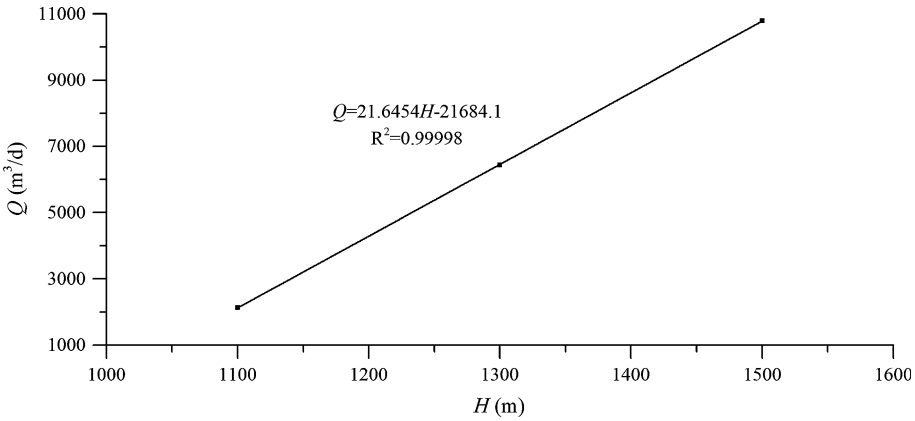

Fig. 12 Fluid flux and fitted curves in Case 3 in which the equivalent hydraulic heads of the left boundary are 1100, 1300 and 1500 m ($1000\ \text{m} < H \leq 1500\ \text{m}$)

nonlinear changes in z direction in a geothermal system of a horizontal, homogeneous and isotropic confined aquifer where the heat flow from below exists, as shown in Fig. 1c. For fluid flux through the vertical flow section, the temperature increases and the dynamic viscosity u decreases, which directly lead to the increase in the fluid flux. When the temperature of the top boundary is 45, 50 and 55 °C, the values of fluid flux through the vertical flow section are 2134, 2214 and 2295 m^3/d in Case 2. When the hydraulic gradient linearly increases, the fluid flux also increases linearly, which is consistent with the aquifer under normal temperature. For the equivalent hydraulic head in x direction, when the temperature difference between the top and bottom boundaries increase, the hydraulic gradient slightly increases with the temperature difference. For example, when the temperature differences are 15, 10, 5 and 0 °C, the hydraulic gradients are 0.01005, 0.01003, 0.01002 and 0.01 in Cases 1 and 2. When the equivalent hydraulic head difference between the left and right boundaries enlarges 3 and 5 times, the equivalent hydraulic heads also decrease linearly and the hydraulic gradient also enlarges 3 and 5 times. For the equivalent hydraulic head in z direction, the equivalent hydraulic head obeys nonlinear changes and increases with the increasing elevation and can be described by using a 2nd order polynomial function. The fitted functions show that when the temperature difference between the top and bottom boundaries is higher, this phenomenon is more obvious. When the temperature difference decreases, the equivalent hydraulic head is close to the linear changes. When the temperature difference is

equal to 0, the equivalent hydraulic head just meet the linear changes in z direction. The numerical results are helpful in understanding the principle of groundwater movement in a thermal groundwater system.

Acknowledgements This work was supported by the Natural Science Foundation of Beijing (8152026), the Fundamental Research Funds for the Central Universities of China (2652013085, 2652014089, 2652015244, 2652015245, 2562015426) and the project of China Geological Survey (1212011120064).

References

Ataie-Ashtiani B, Simmons CT, Werner AD (2014) Influence of boundary condition types on unstable density-dependent flow. Groundwater 52:378–387

Bear J (1972) Dynamics of fluids in porous media. American Elsevier, NewYork

Bear J (1979) Hydraulics of groundwater. McGraw-Hill, London

Brebbia CA, Zamani NG (1987) Boundary element techniques: applications in fluid flow and computational aspects. Computational Mechanics Publications, Southampton

Brooks AN, Hughes TJ (1982) Streamline upwind/Petrov-Galerkin formulations for convection dominated flows with particular emphasis on the incompressible Navier-Stokes equations. Comput Methods Appl Mech Eng 32:199–259

Chen M, Wang J, Deng X (1994) Geothermal resources in China. Science Press, Beijing **(In Chinese)**

COMSOL (2013) COMSOL multiphysics modeling guide (version 4.4). COMSOL AB, Stockholm

Diersch H-JG (2002) About the difference between the convective form and divergence form of transport equation. FEFLOW-White papers, vol I, WASY Ltd, Berlin

Diersch H-JG (2005b) FEFLOW Reference Manual WASY GmbH Institute for Water Resources Planning and Systems Research Ltd, Berlin

Diersch H-JG (2005a) FEFLOW-White papers, vol I. WASY GmbH Institute for Water Resources Planning and Systems Research Ltd, Berlin

Diersch H-JG, Kolditz O (2002) Variable-density flow and transport in porous media: approaches and challenges. Adv Water Resour 25:899–944

Elder J (1967) Transient convection in a porous medium. J Fluid Mech 27:609–623

Harbaugh AW (2005) MODFLOW-2005, the US Geological Survey modular ground-water model: The ground-water flow process US Department of the Interior, US Geological Survey

Heggen RJ (1983) Thermal dependent physical properties of water. J Hydraul Eng 109:298–302

Huang K, Mohanty B, Van Genuchten MT (1996) A new convergence criterion for the modified Picard iteration method to solve the variably saturated flow equation. J Hydrol 178:69–91

Huyakorn PS, Andersen PF, Mercer JW, White HO (1987) Saltwater intrusion in aquifers: development and testing of a three-dimensional finite element model. Water Resour Res 23:293–312

Kipp KL (1987) HST3D: a computer code for simulation of heat and solute transport in three-dimensional ground-water flow systems U.S. Geological Survey, Water-Resources Investigations Report, 86-4095

Li Q, Wang N, Yi D (2005) Numerical analysis. Tsinghua University Press, Beijing **(In Chinese)**

Lin W, Liu Z, Wang W, Wang G (2013) The assessment of geothermal resources potential of China. Geol China 40:312–321

Lusczynski NJ (1961) Head and flow of ground water of variable density. J Geophys Res 66:4247–4256

Nadukandi P, Oñate E, Garcia J (2010) A high-resolution Petrov-Galerkin method for the 1D convection-diffusion-reaction problem. Comput Methods Appl Mech Eng 199:525–546

Ophori DU (1998) The significance of viscosity in density-dependent flow of groundwater. J Hydrol 204:261–270

Post V, Kooi H, Simmons C (2007) Using hydraulic head measurements in variable-density ground water flow analyses. Ground Water 45:664–671

Pruess K, Oldenburg C, Moridis G (1999) TOUGH2 user's guide version 2 earth sciences division. Lawrence Berkeley National Laboratory University of California, Berkeley, California

Putti M, Paniconi C (1995) Picard and Newton linearization for the coupled model for saltwater intrusion in aquifers. Adv Water Resour 18:159–170

Simmons CT, Fenstemaker TR, Sharp JM Jr (2001) Variable-density groundwater flow and solute transport in heterogeneous porous media: approaches, resolutions and future challenges. J Contam Hydrol 52:245–275

Simmons C, Bauer-Gottwein P, Graf T, Kinzelbach W, Kooi H, Li L, Post V, Prommer H, Therrien R, Voss C (2010) Variable density groundwater flow: from modelling to applications. Cambridge University Press, Cambridge

Simpson M, Clement T (2003) Theoretical analysis of the worthiness of Henry and Elder problems as benchmarks of density-dependent groundwater flow models. Adv Water Resour 26:17–31

Smith L, Chapman DS (1983) On the thermal effects of groundwater flow: 1. Regional scale systems. J Geophys Res Solid Earth (1978–2012) 88:593–608

Voss CI (1984) A finite-element simulation model for saturated-unsaturated, fluid-density-dependent ground-water flow with energy transport or chemically-reactive single-species solute transport. US Geological Survey

Voss CI, Souza WR (1987) Variable density flow and solute transport simulation of regional aquifers containing a narrow freshwater-saltwater transition zone. Water Resour Res 23:1851–1866

Wang H (2008) Dynamics of fluid flow and contaminant transport in porous media. Higher Education Press, Beijing, pp 481–484 **(In Chinese)**

Wang X (2011) Groundwater movement equation. Geological Publishing House, Beijing **(In Chinese)**

Wang J, Xiong L, Pang Z (1993) Low-medium temperature geothermal system of convective type. Science Press, Beijing **(In Chinese)**

Woods JA, Carey GF (2007) Upwelling and downwelling behavior in the Elder-Voss-Souza benchmark. Water Resou Res 43

Xue Y, Xie C (2007) Numerical simulation of groundwater. Science Press, Beijing **(In Chinese)**

Zhou X, Chen M, Li C (2001a) 3-Dimensional numerical modeling of geothermal water flow in deep-seated aquifers. Geological Publishing House, Beijing **(In Chinese)**

Zhou X, Chen M, Zhao W, Li M (2001b) Modeling of a Deep-Seated Geothermal System Near Tianjin, China. Ground Water 39:443–448

Zienkiewicz O, Wu J (1992) A general explicit or semi-explicit algorithm for compressible and incompressible flows. Int J Numer Meth Eng 35:457–479